soil systems

MDPI

Article

Constraints to Synergistic Fe Mobilization from Calcareous Soil by a Phytosiderophore and a Reductant

Walter D. C. Schenkeveld *,† and Stephan M. Kraemer

Department of Environmental Geosciences and Environmental Science Research Network, University of Vienna, Althansstrasse 14 (UZA II), 1090 Vienna, Austria; stephan.kraemer@univie.ac.at

* Correspondence: w.d.c.schenkeveld@uu.nl; Tel.: +31-30-253-7631

† Current Address: Copernicus Institute of Sustainable Development, Faculty of Geosciences, Utrecht University, Princetonlaan 8a, 3584 CB Utrecht, The Netherlands.

Received: 6 November 2018; Accepted: 7 December 2018; Published: 16 December 2018

Abstract: Synergistic effects between ligand- and reductant-based Fe acquisition strategies can enhance the mobilization of Fe, but also of competing metals from soil. For phytosiderophores, this may alter the time and concentration window of Fe uptake during which plants can benefit from elevated Fe concentrations. We examined how the size of this window is affected by the ligand and reductant concentration and by non-simultaneous addition. To this end, a series of kinetic batch experiments was conducted with a calcareous clay soil to which the phytosiderophore 2′-deoxymugineic acid (*DMA*) and the reductant ascorbate were added at various concentrations, either simultaneously or with a one- or two-day lag time. Both simultaneous and non-simultaneous addition of the reductant and the phytosiderophore induced synergistic Fe mobilization. Furthermore, initial Fe mobilization rates increased with increasing reductant and phytosiderophore concentrations. However, the duration of the synergistic effect and the window of Fe uptake decreased with increasing reductant concentration due to enhanced competitive mobilization of other metals. Rate laws accurately describing synergistic mobilization of Fe and other metals from soil were parameterized. Synergistic Fe mobilization may be vital for the survival of plants and microorganisms in soils of low Fe availability. However, in order to optimally benefit from these synergistic effects, exudation of ligands and reductants in the rhizosphere need to be carefully matched.

Keywords: Fe acquisition; ligand; metal mobilization; phytosiderophore; reductant; soil; synergistic effect; metal exchange; window of Fe uptake

1. Introduction

Iron (Fe) is an essential micronutrient to plants and most microorganisms [1,2]. Although it is abundant in most environments, it is not always sufficiently bioavailable, particularly in environments with a circumneutral pH, e.g., calcareous soils [3]. Poor Fe bioavailability can lead to Fe deficiency, resulting in reduced primary productivity and yield losses [4,5].

Plants have developed Fe acquisition strategies to cope with low Fe availability [6,7]. These strategies are largely based on classical mineral dissolution mechanisms: proton-promoted dissolution, reductive dissolution and ligand-promoted dissolution [8,9]. So-called Strategy I plants increase proton exudation, exude reductants and upregulate the ferric chelate reductase activity to lower the pH and reduce Fe(III) to the more soluble Fe(II) [2]. Strategy II plants (grasses, including staple crops like wheat, barley, rice and corn) exude chelating ligands called phytosiderophores [10–12]. Phytosiderophores can form soluble complexes with soil-Fe that can readily be taken up by the plant roots [13]. They are exuded in a diurnal pulse release that starts a few hours after the onset of light and last

for a few hours [14,15]. Upon exudation, a time and concentration window of Fe uptake commences during which phytosiderophores increase Fe availability [16]. This window is constrained by the phytosiderophore exudation rate, the solubility of Fe minerals, the Fe mobilization rate, adsorption of the phytosiderophore ligand and its metal complexes, biodegradation of the ligand and complexation of competing metals.

In most studies the reactivity of exuded compounds is examined independently. However, in the plant rhizosphere, exudates are composed of a complex mixtures of compounds [17,18], which may interact, affecting their mutual reactivity [19,20]. For example, the Fe concentration mobilized by compound A and compound B in a combined treatment may be larger than the sum of the Fe concentrations mobilized in separate treatments with A and B. Such non-additive effects are termed 'synergistic Fe mobilization' in the context of this study. Synergistic Fe mobilization in the presence of low molecular weight organic acids (LMWOA) and (phyto)siderophores has been well-documented in goethite model systems [19,21–24] and was recently also examined in soil [25].

In the late 1980s, Stumm and co-workers found that reductants and ligands can also synergistically mobilize Fe in the dissolution of Fe(hydr)oxide minerals [26]. However, these studies were conducted under conditions remote from those under which Fe deficiency occurs. Recently, Wang et al. demonstrated that synergistic Fe mobilization by a ligand and a reductant can also occur at circumneutral pH, under oxic conditions [27]. Subsequent studies demonstrated that the reductant reduces Fe(III) to Fe(II), which can catalyze ligand-controlled dissolution at sub-micromolar Fe(II) concentrations, for a variety of Fe(hydr)oxide minerals and over a broad environmentally relevant pH range [28]. These findings were supported by ATR-FTIR analysis and isotope exchange experiments [29].

Schenkeveld et al. showed for multiple chelating ligands that synergistic metal mobilization by ligands and reductants can also occur in calcareous soil environments (pH 7–8). Synergistic metal mobilization was not only observed for Fe, but also for Co, Ni, Zn and Mn [20]. Metal mobilization rates in combined treatments were particularly enhanced in the first minutes to hours of interaction with the soil.

Synergistic Fe mobilization in the presence of ligands and reductants may be vital for the survival of plants and microorganisms in soils with low Fe availability. In the present study we focus on synergistic Fe mobilization involving phytosiderophores, because of the wide occurrence of grasses, their importance in food production and their potential to provide other plant species with Fe in natural and agricultural ecosystems [30,31]. Reductants in the rhizosphere of grass roots may be exuded by roots of Strategy I plants [32] growing in close proximity, microorganisms [1,33,34] inhabiting the rhizosphere, or possibly also by the grasses themselves. A new class of root exudates with reducing properties called coumarins have recently been identified [35–37], and research on which species exude these compounds is ongoing.

For phytosiderophores, synergistic Fe mobilization from soil proved transient; the synergistic phase was followed by an antagonistic phase, in which the combined ligand and reductant treatment mobilized less Fe than the sum of the separate reductant and ligand treatments [20]. This resulted from enhanced mobilization of competing metals like Ni and Co, which formed more stable metal-phytosiderophore complexes and outcompeted Fe faster under these specific soil conditions.

In the current study, we hypothesize that the size and duration of the synergistic effect in soils may be highly sensitive to the phytosiderophore and the reductant concentration and that the transient nature of synergistic Fe mobilization is related to complexation of competing metals and the depletion of the free ligand. In this sense, we are testing the application of the concept of a time and concentration window of Fe uptake that is enlarged by fast Fe mobilization rates, but diminished by processes such as competitive metal complexation and other loss terms. Also, we hypothesize that a non-simultaneous release of reductant and phytosiderophore will diminish the synergistic mobilization of Fe and the window of Fe uptake.

To test these hypotheses, we examined metal mobilization and the reductant concentration in a series of kinetic batch experiments with a calcareous clay soil to which the phytosiderophore 2′-deoxymugineic acid (*DMA*) and the reductant ascorbate were added.

2. Materials and Methods

2.1. Materials

Soil—The top layer (0–20 cm) of a calcareous clay soil from Santomera (Murcia, Spain) was sampled. This soil has a low reactive Fe content (ammonium oxalate extractable Fe: 0.5 g kg^{-1}) and bioavailable Fe content (DTPA-extractable: 4.9 mg kg^{-1}) and has been used in multiple studies on Fe deficiency in Strategy I and II plants [15,38]. The soil was air-dried and sieved over 2 mm. It has a pH of 7.8, a clay content of 30%, a calcium carbonate content of 50% and soil organic matter content of 1.5%. Selected soil parameters are presented in Table A1.

Chemicals—The ammonium salt of 2′-deoxymugineic acid (*DMA*) was synthesized in accordance with Namba et al. [39] with a purity larger than 95% as determined by H-NMR. Ascorbic acid was purchased from Merck. Ascorbate can be exuded by plants roots [40] and has been used as a model reductant in this study. Ascorbate solutions were prepared freshly directly before application. Both ascorbate and *DMA* readily dissolved in water. Analytical grade chemicals and ultra-pure water were used for preparing experimental solutions. The pH of experimental solutions was adjusted to the range 5–9; the buffer capacity of the soil brought the experimental solutions to soil pH.

2.2. General Experimental Procedure

Experiments were done in 50-mL polypropylene tubes (Greiner bio one) in a soil-solution ratio (SSR) of 1 (kg L^{-1}) with 10 mM $CaCl_2$ as background electrolyte. The influence of microbial activity on metal mobilization was examined by including treatments with and without a sterilant (0.2 g L^{-1} Bronopol). Bronopol does not affect mobilization of metals by *DMA* from Santomera soil [41]. Blank treatments without addition of *DMA* or ascorbate were also included. Soil samples were pre-equilibrated with electrolyte solution (and sterilant, when required) for two days at 90 percent of the final solution volume, prior to addition of ascorbate and *DMA*, to prevent fast mobilization of labile metal pools generated during soil drying [42]. Samples were placed in an end-over-end shaker rotating at 18 rpm in the dark at 20 ± 1 °C. Sampling was done in a sacrificial manner after 0.25, 0.5, 1, 2, 4, 8, 24, 48, 96 and 168 h, except in the '*ascorbate residence time in soil solution*' experiment, after 0.083, 0.25, 0.5, 1 and 4 h, and the 'varying ligand and reductant concentration' experiment, after 0.25 h. Samples were centrifuged for 3 min at 4500 rpm and filtered over 0.45 µm cellulose acetate filters (Whatman Aqua 30/0.45 CA). The pH of the filtrate was measured and the filtrate was further analyzed.

2.3. Experiments

Ascorbate residence time in soil solution—To assess the time frame during which ascorbate reduces soil constituents, the residence time of ascorbate in soil solution was examined. 1 mM Ascorbate was added to Santomera soil and the soil solution was sampled over time. After filtration, the ascorbate concentration was determined spectrophotometrically.

Lag time between addition of reductant and chelating ligand—To investigate if metal mobilization by phytosiderophores that are released in a diurnal pulse may be affected by reductants that have been released before the phytosiderophores exudation pulse, we investigated the effect of a lag time between PS and reductant additions on metal mobilization as a function of time. 1 mM ascorbate was added, either simultaneously, or one or two days prior to a 100 µM *DMA* addition. The moment of *DMA* addition was set to $t = 0$; ascorbate was added at either $t = -48$ h, $t = -24$ h or $t = 0$.

Varying reductant concentration—The influence of the reductant concentration on metal mobilization in the presence of a phytosiderophore was examined as a function of time. For this purpose ascorbate (0, 0.1, 0.3 or 1.0 mM) and *DMA* (100 µM) were added simultaneously to Santomera soil.

Effect of microbial activity—Biodegradation may reduce the effectiveness of iron mobilizing exudates over time, essentially closing the concentration window of Fe uptake. The effect of biodegradation on this window was examined by repeating the *varying reductant concentration* experiment, yet without addition of Bronopol.

Varying ligand concentration—The influence of the phytosiderophore concentration on metal mobilization in presence of a reductant was examined as a function of time. For this purpose *DMA* (10, 30 or 100 μM) and ascorbate (0 or 1 mM) were added simultaneously to Santomera soil.

Varying ligand and reductant concentration—The possibility of synergistic Fe mobilization at naturally occurring phytosiderophore concentrations was examined, and the phytosiderophore to reductant ratio for optimizing Fe mobilization was assessed, by varying both the phytosiderophore and the reductant concentration for a single interaction time. Ascorbate (0, 0.05, 0.1, 0.2 and 0.3 mM) and *DMA* (0, 10, 20, 30 and 50 μM) were added to Santomera soil simultaneously in all combinations of concentrations and interacted for 0.25 h.

2.4. Analysis

Metal concentrations (Fe, Cu, Ni, Co, Zn, Mn and Ca) were determined by ICP-OES (Optima 5300 DV, PerkinElmer). Samples were acidified with nitric acid prior to analysis. Mobilized metal concentrations were calculated as the difference in metal concentration between the treatment involving a ligand or a reductant (or both) and the corresponding blank treatment.

Ascorbate concentrations were determined spectrophotometrically with methylene blue. The decolorization rate of methylene blue by reduction relates logarithmically to the ascorbate concentration in solution. Samples were acidified to 0.5 M HCl and methylene blue was added to a concentration of 10 μM. Absorbance was measured at 665 nm with a photospectrometer (Varian Cary 50), 60 s after addition of the methylene blue. This short reaction time was chosen to minimize the re-oxidation of methylene blue with atmospheric oxygen. Calibration standards were prepared using soil extract to match the matrix with the experimental samples, and the redox buffer capacity of DOC present in soil solution was accounted for.

3. Results and Discussion

3.1. Ascorbate Residence Time in Soil Solution

To quantitatively assess time scales of ascorbate interactions with soil, ascorbate was added to a soil suspension and the remaining ascorbate concentration in the soil solution was examined as a function of time. After application of 1 mM ascorbate its concentration dropped to near the limit of quantification (0.02 mM) within 0.083 h (5 min) and further decreased to background level in the following 10 min (Table A2 and Figure A1). Although losses from solution related to ascorbate adsorption to soil surfaces cannot be excluded, these results suggest that the reaction of ascorbate with the soil was near instantaneous and complete. This is consistent with previous observations of strong initial mobilization of several metals after combined additions of ligands and ascorbate [20].

3.2. Lag Time between Addition of Reductant and Chelating Ligand

To investigate a potential memory effect from reductants after their loss of reactivity (as observed in the previous experiment) on metal mobilization by chelating ligands, we performed experiments where 100 μM *DMA* was added one or two days after application of 1 mM ascorbate. By itself, ascorbate (ascorbate-only treatment) did not mobilize metals from Santomera soil to a substantial degree, except for Mn (Figure 1). Potential formation of new mineral phases as a result of ascorbate addition was not examined spectroscopically; equilibrium modeling with PhreeqC using the Minteq database suggested no saturation of Fe(II) or Mn(II) carbonate minerals had occurred (data not shown).

Despite the high reactivity and short residence time of ascorbate in soil, synergistic mobilization of Fe, Ni, Co and Zn was still observed when *DMA* was applied one or two days after the

ascorbate (Figures 1 and A2). This demonstrates that ascorbate-induced changes in metal speciation, and enhanced availability of Fe and other metals for complexation by *DMA* were preserved far beyond the residence time of ascorbate in the soil. It implies that exudation of reductants and phytosiderophores does not have to be simultaneous in order for plants to benefit from synergistic Fe mobilization.

In all treatments with *DMA*, mobilized Fe concentrations first increased, reached a maximum and then decreased. This time course of Fe mobilization represents the concentration window during which Fe availability to plants and microorganisms is enhanced. Synergistic Fe mobilization, defined as a more than additive mobilization of Fe in the presence of the ligand and the reductant, is a process that may potentially increase the size of the window. For all treatments with *DMA* and ascorbate, an initial synergistic effect was observed. The maximum synergistic effect was reached after 1 h and the size of the effect decreased with increasing lag-time between applications. The synergistic effect disappeared between 4 and 8 h after *DMA* application, after which Fe mobilization became antagonistic. The interaction time during which Fe concentrations increased was positively correlated to increasing lag times and was longest when no ascorbate was added (Figure 1a).

A prominent feature of the time and concentration window is the maximum soluble Fe concentration. Counter-intuitively, ascorbate additions diminished the observed maximum mobilized Fe concentrations compared to the *DMA*-only treatment. After the respective maximum Fe concentrations were reached in the treatments with ascorbate addition, Fe concentrations converged over time. Compared to the *DMA*-only treatment, the window of Fe uptake was reduced by the presence of the reductant in all treatments containing ascorbate. However, during the first hour after *DMA* addition over 60 and 40% additional Fe were mobilized in the treatments with a lag time of one or two days, respectively, compared to the *DMA*-only treatment (Figure 1a). In view of processes like biodegradation, which may be accelerated in rhizosphere soil due to high microbial activity, and thereby may further limit the lifetime of phytosiderophore ligands in the soil, Fe mobilization in the first few hours may be of high importance in plant Fe acquisition.

As discussed above, the window of Fe uptake may be reduced by metal exchange processes leading to the loss of soluble Fe*DMA* and increasing concentrations of competing metal complexes over time. In treatments with *DMA*, Ni and Co concentrations increased throughout the experiment. A considerable synergistic effect in Ni and Co mobilization by *DMA* and ascorbate was observed in experiments with simultaneous additions and in treatments with a one- or two-day lag phase between the applications (Figure 1b,c). Puschenreiter et al. (2017) demonstrated that enhanced phytosiderophore exudation by wheat plants increased Ni mobilization and uptake from certain soils [43]; similarly, synergistic Ni mobilization may also enhance Ni uptake. Ni and Co concentrations converged over time in treatments with *DMA* and ascorbate. Similar to Fe mobilization, the initial mobilization rates for Ni and Co were smaller in the combined treatments with a lag phase compared to simultaneous application. This resulted in a slower depletion of the free *DMA* ligand concentration, and consequently a later onset of competitive exchange with Fe, explaining why maximum Fe mobilization was reached later. The lag phase decreased Ni and Co mobilization rates less strongly than Fe mobilization rates, resulting in lower maximum mobilized Fe concentrations in the treatments with a lag phase.

As previously reported, Cu and Zn mobilization were not strongly affected by application of ascorbate in addition to *DMA* [20] (Figure A2). Mn mobilization was mainly affected by ascorbate addition. Differences in mobilized Mn concentrations between treatments (Figure 1d) largely resulted from defining $t = 0$ as the moment of *DMA* addition rather than ascorbate addition (except in the ascorbate-only treatment where $t = 0$ corresponds with the moment of ascorbate addition). In Figure A3 Mn mobilization data are presented with $t = 0$ corresponding with the moment of ascorbate addition for the ascorbate-only and the combined ascorbate and *DMA* treatments. It illustrates that synergistic Mn mobilization upon *DMA* addition is small and short-lived.

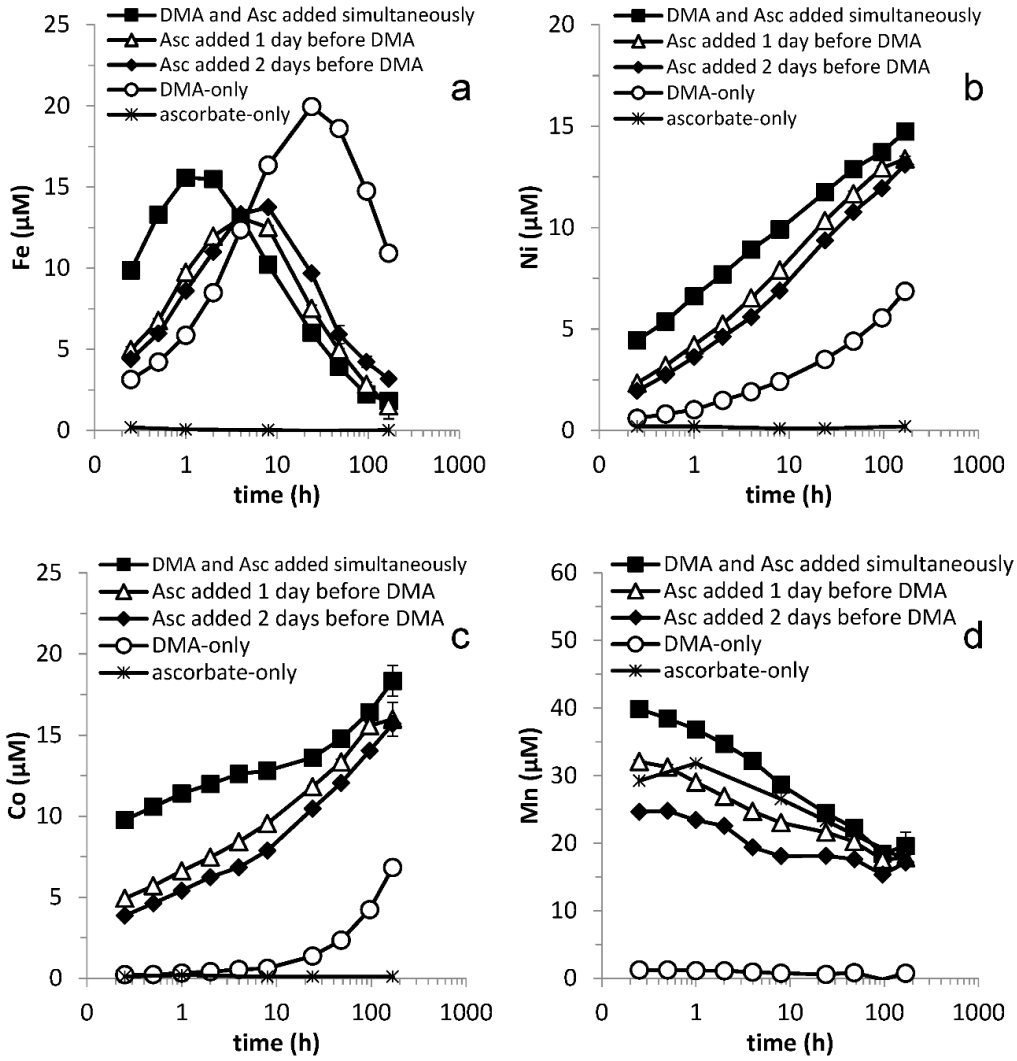

Figure 1. Mobilization of (**a**) Fe, (**b**) Ni, (**c**) Co and (**d**) Mn from Santomera soil as a function of time by 100 µM *DMA* and 1 mM ascorbate (SSR = 1; 10 mM $CaCl_2$; 0.2 g L^{-1} Bronopol). In combined treatments, *DMA* was applied simultaneously, one or two days after the ascorbate application. t = 0 corresponds to the time of *DMA* addition, except in the ascorbate only experiment where t = 0 corresponds to the time of ascorbate addition. Error bars indicate standard deviations.

Enhanced metal mobilization in treatments with combined application of ascorbate and *DMA* may result from reductive dissolution of minerals with which these metals were associated. The strong increase in Mn concentration suggests that Mn(hydr)oxide minerals strongly compete with Fe bearing phases as electron acceptor in ascorbate oxidation leading to reductive dissolution of these minerals. Ni and Co are known to associate strongly with Mn(hydr)oxide minerals [44,45], and Fe can also be incorporated in such minerals [46]. Re-oxidation of Mn is kinetically slow [47], as illustrated by the slow decline in Mn concentration, therefore metals are not quickly reincorporated and may remain more available for complexation for a longer period. Reduction of surface metal ions of metal(hydr)oxides by ascorbate may also lead to electron transfer and atom exchange (ETAE) [48] which can release substituted metals from the crystal lattice [49,50] and make them available for complexation by *DMA*. Furthermore, reductive dissolution of crystalline Fe(hydr)oxide minerals and subsequent oxidative re-precipitation in the presence of humic substances can result in the formation of poorly crystalline Fe minerals [51], that are more readily complexed by *DMA*. The decline in synergistic effect with increasing lag time may in part be due to a slow recrystallization [52], making Fe gradually less

available for complexation. It was however recently reported that Fe mineral association with humic substances [53] or with ascorbate [54] may hinder recrystallization even in the presence of Fe(II).

It should be noted that the experiments were done in the presence of atmospheric oxygen in the headspace of the batch reactors in order to mimic the conditions in aerated soil where iron limitation typically occurs. Therefore, oxygen will ultimately re-oxidize Fe(II) and Mn(II) as transient intermediates. In contrast to Mn(II), the re-oxidation of Fe(II) is rapid under oxic conditions at non-acidic pH, particularly in the presence Fe(hydr)oxide mineral surfaces [55]. Therefore it is improbable that the synergistic Fe mobilization observed after a lag phase of one or two days is related to transient Fe(II) concentrations.

3.3. Varying Reductant Concentration

The effect of the reductant concentration on the synergistic effect and the window of Fe uptake was examined in a series of experiments in which the ascorbate concentration was varied for a fixed *DMA* concentration.

Initially, mobilized Fe concentrations in treatments with *DMA* increased with increasing ascorbate concentration added (Figure 2a); differences between the treatments with 0.3 and 1 mM ascorbate were, however, small. The time required for the mobilized Fe concentration to reach a maximum decreased with increasing ascorbate concentration; from 24 h for 0.1 and 0 mM ascorbate to 1 h for 1 mM ascorbate. Subsequently, the mobilized Fe concentration declined. Also the duration of synergistic Fe mobilization decreased with increasing ascorbate concentration (from 24 h with 0.1 mM to 4 h with 1 mM). The maximum synergistically enhanced Fe concentration, however, increased with increasing ascorbate concentration and was over three times larger for 1 mM than for 0.1 mM ascorbate. For all ascorbate concentrations, ~65% of the maximum synergistically enhanced Fe concentration was already reached after 0.25 h. While we investigated the effect of ascorbate concentrations in the absence of *DMA*, we observed negligible metal (including Fe) mobilization except for Mn and we only represent the 1 mM ascorbate treatment for comparison in Figure 2.

In the presence of *DMA*, mobilized Ni and Co concentrations increased throughout the experiment and were consistently larger in treatments with larger applied ascorbate concentrations (Figure 2b,c). Differences in mobilized Ni concentrations between these treatments increased up to 48 h, after which they mildly decreased. Approximately 40% of the maximum synergistically enhanced Ni concentration was reached after 0.25 h for all ascorbate concentrations. Differences in Co mobilization between these treatments increased up to 96 h, except for differences relative to the 1 mM ascorbate, which reached a maximum after 4 h and declined after that. The fraction of the maximum synergistically enhanced Co concentration reached after 0.25 h ranged from ~30% for 0.1 mM ascorbate to ~75% for 1.0 mM ascorbate

For Mn, ascorbate largely governed the mobilized concentrations; the contribution from *DMA* was subordinate. Both the initial Mn mobilization and the subsequent rate of decline in Mn concentration were proportional to the applied ascorbate concentration, in the absence as well as in the presence of *DMA*. The synergistic effect in Mn mobilization decreased from 0.25 h on and had become marginal after 24 h. Ascorbate only had a minor effect on Cu mobilization by *DMA* (Figure S4a). Zn mobilization by *DMA* was only substantially affected by the highest applied ascorbate concentration (1 mM) (Figure S4b); in this treatment a small initial synergistic effect changed after 8 h into antagonistic effect.

For Fe, Ni, Co and Mn, the initial mobilization rates (from t = 0 to 0.25 h) were linearly related to the applied ascorbate concentration (Figure 3); for Mn this was the case both in presence and absence of *DMA*, for Fe, Ni and Co mobilization in absence of *DMA* was negligible. The intercepts in Figure 3 corresponds with ligand-promoted dissolution rate. For Ni, Co and Mn the linear relation held for the entire applied ascorbate concentration range, for Fe up to 0.3 mM, after which a plateau was reached. This could suggest that Fe originates from a different source in the soil than Ni, Co and Mn (i.e., Mn-oxide minerals). These linear relations demonstrate that initial mobilization of the aforementioned metals from Santomera soil is first order in the applied ascorbate concentration. The slopes of the linear fits are a measure for the responsiveness of the initial mobilization rate to the ascorbate concentration.

Until the plateau was reached, Fe was more sensitive to synergistic mobilization than the competing metals Ni and Co (Figure 3). Beyond 0.3 mM ascorbate addition, the additional gain in synergistic Fe mobilization was small (Figures 2a and 3), but mobilization of Co and Ni continued to increase (Figure 2b,c), leading to a considerably faster onset of competitive displacement of Fe from Fe*DMA* by Ni and Co and subsequent decline in the mobilized Fe concentration. This demonstrates that once an optimum reductant concentration was reached, further addition had a detrimental effect on the size of the window of Fe uptake.

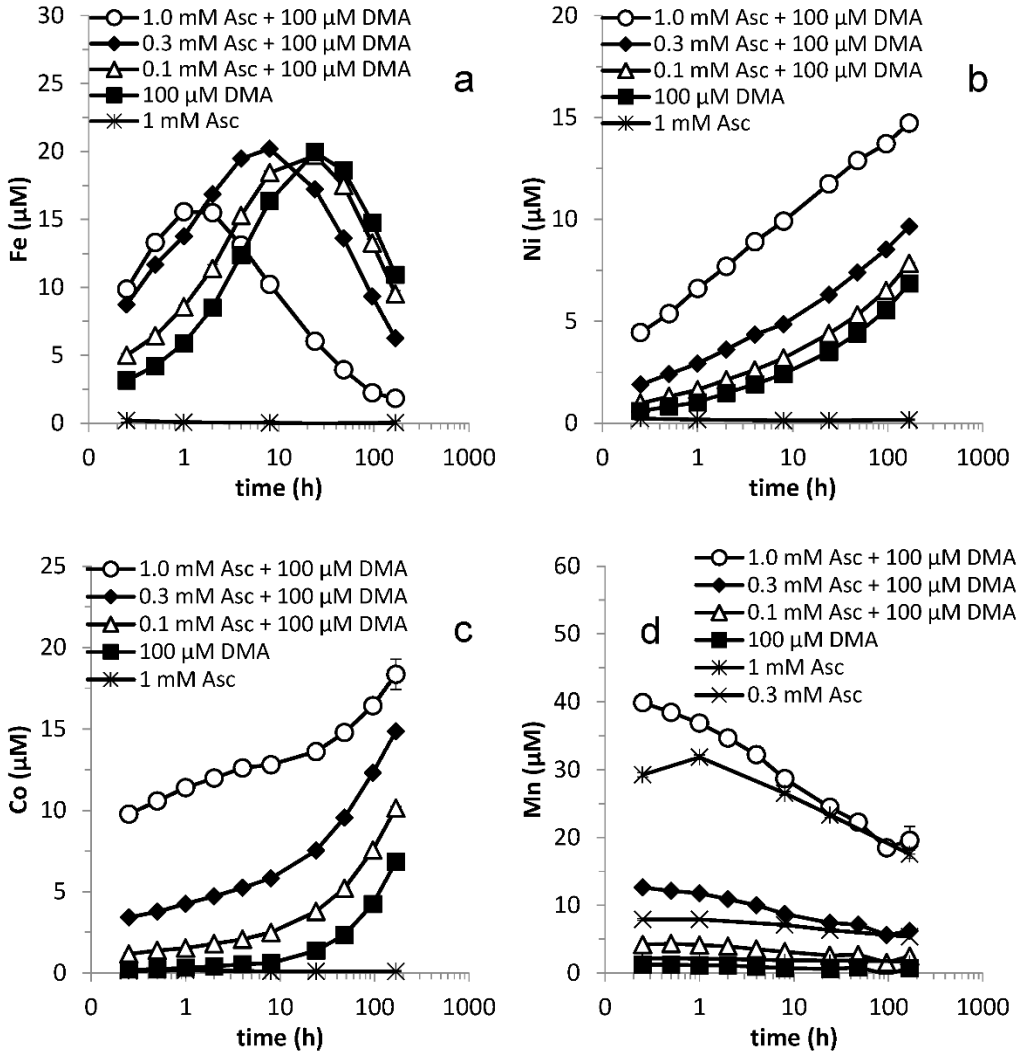

Figure 2. Mobilization of (**a**) Fe, (**b**) Ni, (**c**) Co and (**d**) Mn from Santomera soil as a function of time by 100 µM *DMA* and various ascorbate concentrations (0.1, 0.3 and 1.0 mM) (SSR = 1; 10 mM $CaCl_2$; 0.2 g L^{-1} Bronopol). Error bars indicate standard deviations.

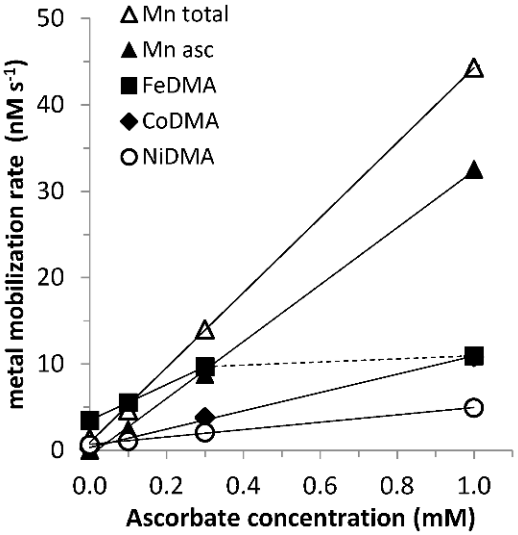

FeDMA*	$R = 20.7\ 10^{-6}$ [asc] + $3.5\ 10^{-9}$	$R^2 = 1$
NiDMA	$R = 4.3\ 10^{-6}$ [asc] + $0.7\ 10^{-9}$	$R^2 = 0.997$
CoDMA	$R = 10.6\ 10^{-6}$ [asc] + $0.3\ 10^{-9}$	$R^2 = 0.998$
Mn total$	$R = 43.4\ 10^{-6}$ [asc] + $0.9\ 10^{-9}$	$R^2 = 0.999$
Mn asc§	$R = 32.9\ 10^{-6}$ [asc] - $0.6\ 10^{-9}$	$R^2 = 0.999$

* only 0, 0.1 and 0.3 mM ascorbate were included

$ DMA + ascorbate treatment

§ ascorbate-only treatment

Figure 3. Initial metal mobilization rates (0–0.25 h) from Santomera soil as a function of the applied ascorbate concentration. Error bars indicate standard deviations.

3.4. Effect of Microbial Degradation

Microbial degradation constrains the residence time of phytosiderophores in the rhizosphere [56] and hence the window of Fe uptake [16]; the duration of the synergistic effect cannot extend beyond this. In treatments where microbial activity had not been suppressed, *DMA*-mediated Fe mobilization reached background values within 24 h as a result of *DMA* ligand degradation (Figure 4), while in the *DMA*-only treatment with Bronopol, the mobilized Fe concentration reached its maximum after this time. In view of the time constraint imposed by microbial degradation, Fe mobilization faster than in the *DMA*-only treatment is favorable for the size of the window of Fe uptake (e.g., 0.3 mM ascorbate + 100 mM *DMA*), as long as the negative impact from enhanced mobilization of competing metals leading to Fe displacement from Fe*DMA* complexes does not exceed the gain (e.g., 1.0 mM ascorbate + 100 mM *DMA*) (Figure 4).

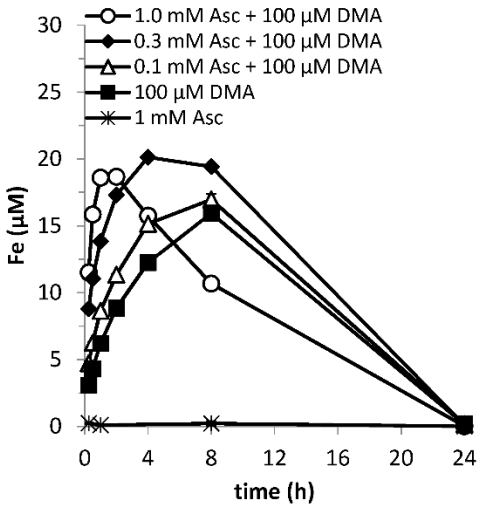

Figure 4. Mobilization of Fe from Santomera soil (SSR = 1; 10 mM $CaCl_2$) as a function of time by 100 µM *DMA* and various ascorbate concentrations (0.1, 0.3 and 1.0 mM) in absence of a sterilant. Error bars indicate standard deviations.

3.5. Varying Ligand Concentration

Concentrations of exuded ligands may vary over short spatial distances in the rhizosphere. In this context we investigated the effect of ligand concentration on iron mobilization at a fixed ascorbate concentration of 1 mM (Figure 5a). We observed synergistic Fe mobilization for up to 4 h in the presence of 100 µM *DMA*. In the presence of 30 and 10 µM *DMA*, an antagonistic effect was observed from the first time point on (0.25 h) and Fe mobilization was negligible. In contrast, substantial Fe mobilization was observed in the corresponding *DMA*-only treatments. In previous studies a faster depletion of the free *DMA* ligand and an earlier onset of competitive displacement of Fe from Fe*DMA* had been observed for smaller applied *DMA* concentrations [16,42]. Similarly, in the treatments with 10 and 30 µM *DMA*, a strong enhancement in availability of competing metals due to ascorbate addition relative to the amount of ligands available for complexing these metals can dramatically enhance competitive metal exchange reactions. This is illustrated by strongly enhanced mobilization of Ni and Co that was observed for all applied *DMA* concentrations for the entire duration of the experiment (Figure 5b,c). Ni was the only metal for which the concentration increased throughout the experiment in all treatments, consistent with the predicted *DMA* equilibrium speciation for Santomera soil [57]. The synergistic effect for Ni reached a plateau after approximately 24 h. In all treatments without ascorbate and in the combined treatment with 100 µM *DMA* and ascorbate, Co concentrations increased continuously. In the combined treatments with 10 and 30 µM *DMA*, the mobilized Co concentration declined after a rapid initial mobilization. Co was effectively displaced from Co*DMA* by Ni and Cu. This decline in Co concentration coincided with a decline in Mn concentration (Figure 5d), which was observed in all treatments where ascorbate was applied. Co liberated by reductive dissolution of Mn-oxide minerals may re-associate with freshly forming Mn-oxide minerals during slow re-oxidation of soluble Mn(II). Also, the slow oxidation of Co(II) to Co(III) at these Mn-oxide surfaces [58] may reduce Co activity, facilitating competitive displacement of Co from Co*DMA*. For Mn a synergistic effect was only observed with 100 µM *DMA*; at lower *DMA* concentrations, Mn mobilization was entirely controlled by the ascorbate. For both Cu and Zn mobilization, combined ascorbate and *DMA* application generated a temporary synergistic effect with 100 µM *DMA*, but an antagonistic effect with 10 and 30 µM *DMA* from 0.25 h onward, similar as for Fe mobilization (Figure 5e,f).

These observations suggest that the mobilization of competing metal ions may reduce the duration of (synergistic) Fe mobilization to the extent that plants may no longer be able to benefit from the ligands they exude. It underlines that matching the exuded amounts of ligand and reductant into the rhizosphere is critical.

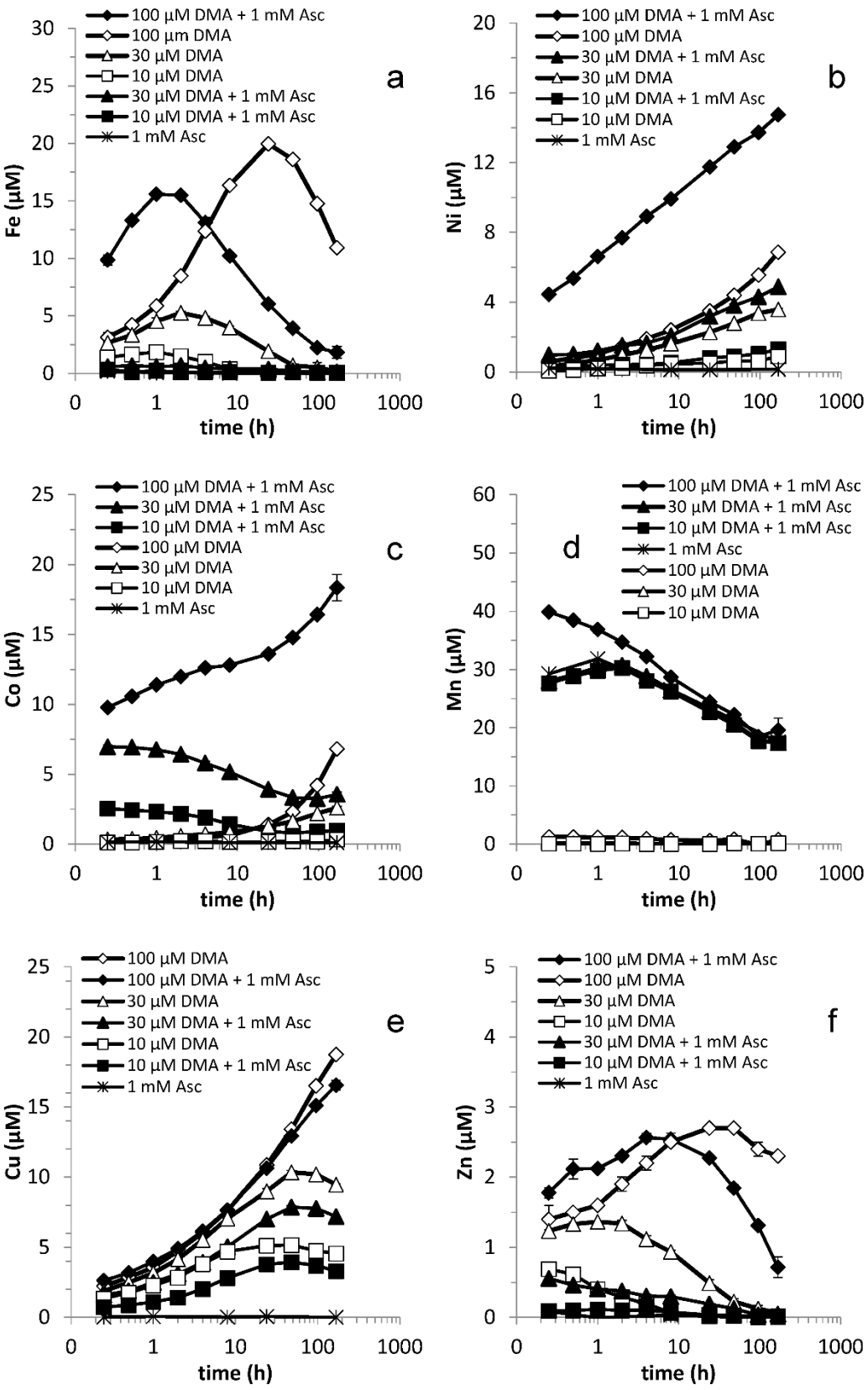

Figure 5. Mobilization of (**a**) Fe, (**b**) Ni, (**c**) Co, (**d**) Mn, (**e**) Cu and (**f**) Zn from Santomera soil as a function of time by 0, 10 µM, 30 µM, and 100 µM *DMA* in presence or absence of 1 mM ascorbate (SSR = 1; 10 mM $CaCl_2$; 0.2 g L^{-1} Bronopol). Error bars indicate standard deviations.

3.6. Varying Ligand and Reductant Concentration

The results from the *Varying ligand concentration* experiment raise the question if synergistic Fe mobilization is in fact possible in Strategy II Fe acquisition: in experiments with wheat plants grown on calcareous soils, phytosiderophore pore water concentrations were in the lower micromolar range [15], while no synergistic Fe mobilization was observed for up to 30 µM *DMA* due to enhanced Ni and Co mobilization (Figure 5). However, the total phytosiderophore concentration (solid + solution) might be up to an order of magnitude larger than the pore water concentration as a result of adsorption [42,59]. Also, phytosiderophore concentrations in the rhizosphere are presumably larger than the pore water average [60]. Furthermore, the 1 mM ascorbate concentration proved excessive for generating synergistic Fe mobilization in the aforementioned pore water phytosiderophore concentration range on the timescales examined. Therefore, the potential for synergistic Fe mobilization with naturally occurring phytosiderophore concentrations was examined by varying the phytosiderophore concentration (in the range of tens of micromolars), as well as the ascorbate concentration (in the range of tenths of millimolars). Metal mobilization was examined after a short interaction time (0.25 h) to minimize the effect of competitive Fe displacement from Fe*DMA* complexes.

Synergistic Fe mobilization was observed for the entire tested *DMA* concentration range (10–50 µM), increasing the mobilized Fe concentration by up to 25% for 10 µM *DMA* and by up to 100% for 20 µM *DMA* (Figure 6a). The ascorbate concentration for which synergistic Fe mobilization was largest increased with increasing *DMA* concentration, from 0.1 mM for 10 µM *DMA* to 0.2 mM ascorbate for 20 µM *DMA*, while for higher *DMA* concentrations no maximum was reached yet. For 10 µM *DMA* combined with 0.3 mM ascorbate an antagonistic effect was found already after 0.25 h.

Rate laws were developed to quantitatively describe the kinetics of metal mobilization from soil. Recently, Kang et al. captured the catalytic effect of Fe(II) on ligand-promoted dissolution of Fe(hydr)oxide minerals in a rate-law equation:

$$R_{net} = R_L + R_{cat} = k_{L,}\,[L]_{ads} + k_{Fe(II)}[Fe(II)]_{ads}\,[L]_{ads} \quad (1)$$

in which R_{net} is the net dissolution rate, R_L is the ligand–promoted dissolution rate, R_{cat} is the rate enhancement due to Fe(II) catalysis, k_L is the rate coefficient of ligand-controlled dissolution, $[L]_{ads}$ is the adsorbed ligand concentration, $k_{Fe(II)}$ is the rate coefficient associated with the effect of Fe(II) on ligand-controlled dissolution and $[Fe(II)]_{ads}$ is the adsorbed (II) concentration. In this previous study, Fe(II) was used as reductant of Fe(III) in the mineral structure and no net reduction of Fe occurred. In the present study, net reduction of metals in the soil by a reductant (ascorbate) and subsequent reductive dissolution occurs, which has to be included in an expanded conceptual model describing net mobilization rates (R_{net} ([mol L^{-1} s^{-1}])). In this expanded conceptual model we assume linearly additive contributions from the ligand-only (R_L), from the reductant-only (R_R) and from the synergism between the two (R_{syn}):

$$R_{net} = R_L + R_R + R_{syn} \quad (2)$$

Because soils are multi-phase systems, they generally will not conform to mechanistic rate laws describing surface-controlled ligand-promoted or reductive dissolution as developed previously for pure iron oxides, e.g., by Banwart et al. Instead, for soils we described the rate as a function of applied concentrations:

$$R_{net} = k_{DMA}[DMA]^a + k_{asc}[ascorbate]^b + k_{syn}[ascorbate]^c[DMA]^d \quad (3)$$

in which k_{DMA}, k_{asc}, k_{syn} are the conditional rate constants for metal mobilization by *DMA*-only [s^{-1}], ascorbate-only [s^{-1}] and for synergistic metal mobilization by ascorbate and *DMA* [L s^{-1} mol^{-1}], respectively, and a, b, c and d are the rate orders. For the *DMA* ligand, overall adsorption to Santomera soil is linearly related to the applied concentration [59]; however, the distribution of the ligand over reactive surfaces in the soil and the role of ligand exchange reactions with natural organic matter (NOM) in relation to metal mobilization remain unspecified.

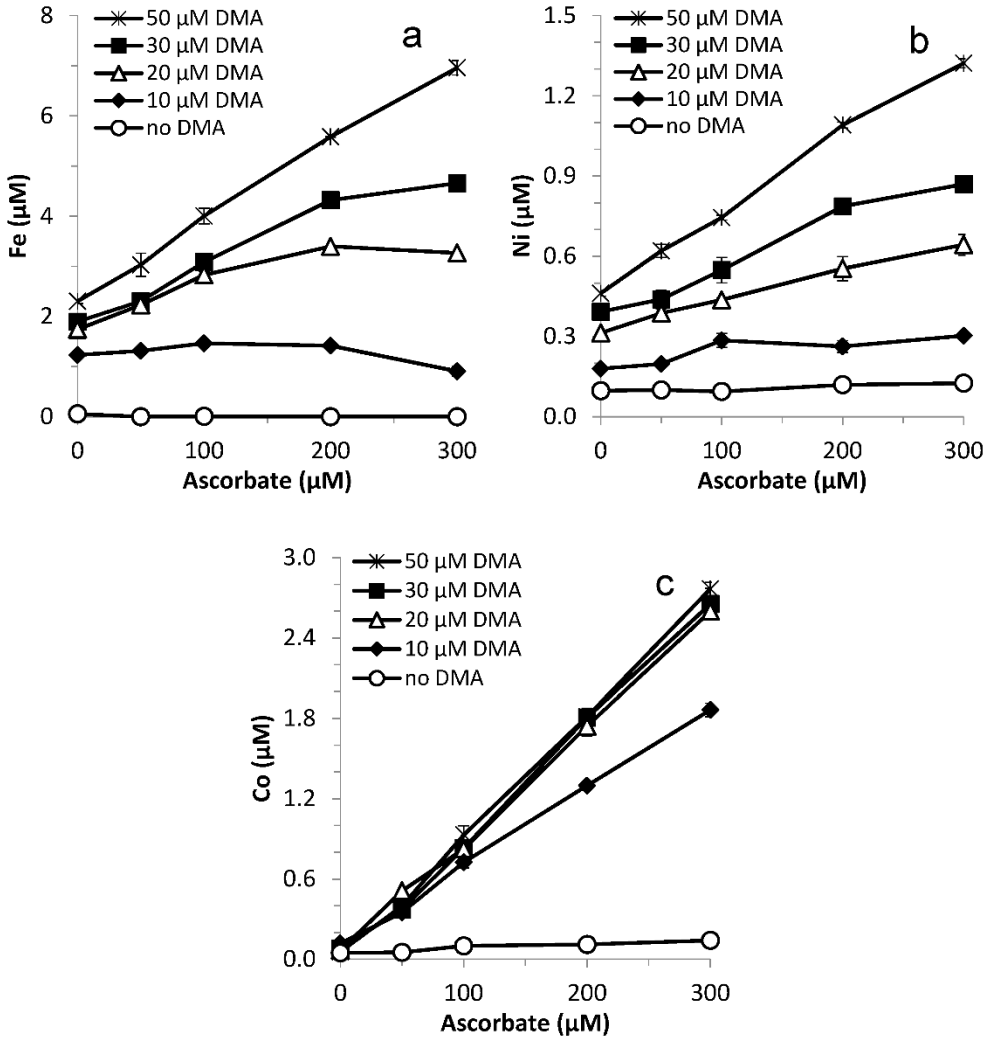

Figure 6. Mobilized (**a**) Fe, (**b**) Ni and (**c**) Co concentrations from Santomera soil by 0, 10, 20, 30 and 50 µM *DMA* as a function of ascorbate concentration (SSR = 1; 10 mM $CaCl_2$; 0.2 g L^{-1} Bronopol) after 0.25 h. Error bars indicate standard deviations.

Experimentally observed mobilized metal concentrations after 0.25 h (Figure 6) were converted into average initial mobilization rates (Figure 7) by dividing them by 900 s. Rate constants k_{DMA}, k_{asc} and k_{syn} and rate orders *a*, *b* and *c* were fit to these rates (R_{net}; Equation (3)) for the individual metals (Table 1) using the Excel solver. k_{asc} and b were only fit for Mn, because it was the only metal showing an increase in solution concentration in the ascorbate-only treatments. For Fe, Ni, Co and Mn rate order *d* was fixed at 1, based on the results from the varying reductant concentration experiment. For Mn, Cu and Zn the concentration data did not indicate a synergistic effect (Figure A4). For these metals, k_{syn} and c were not fit. Only rates from treatments unaffected by competitive displacement (i.e., for which the mobilized Fe concentration increased linearly with the applied ascorbate concentration for a fixed *DMA* concentration; Figure 6a) were included in the fitting (12 in total; Table S3). For comparison, rates calculated with the fitted parameters are included in red in Figure 7. The excellent agreement between measured and calculated rates shows in the high R^2 values and the tangents close to 1 of the linear regressions between the two (Table 1).

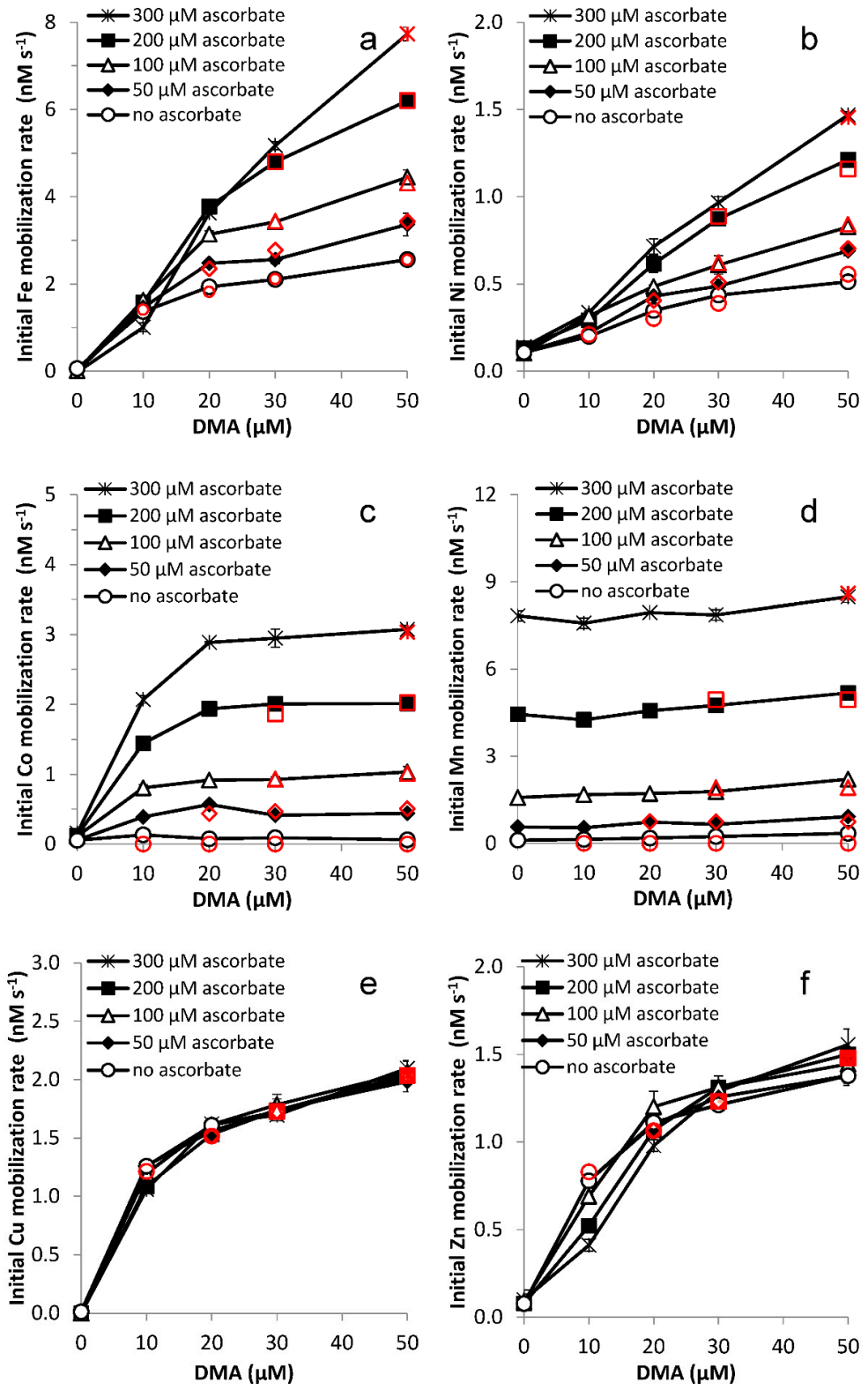

Figure 7. Average mobilization rate (0–0.25 h) for (**a**) Fe, (**b**) Ni, (**c**) Co, (**d**) Mn, (**e**) Cu and (**f**) Zn from Santomera soil as a function of *DMA* concentration for various ascorbate concentrations (SSR = 1; 10 mM $CaCl_2$). Black markers indicate measured rates, red markers represent the corresponding rates calculated from rate Equation (3) using the fitted rate constants and rate orders presented in Table 1. Rates were only calculated for treatments included in the fitting (Table S3); for the rationale on inclusion of treatments, see the main text. Error bars indicate standard deviations.

Table 1. Conditional rate constants and rate orders for rate Equation (3), describing metal mobilization from Santomera soil by *DMA* and ascorbate (simultaneously applied; 10 mM $CaCl_2$; 20 °C; SSR = 1). Rate constants and rate orders were derived by fitting experimental rate data from 12 treatments in which no competitive Fe displacement occurred (Table A3) to Equation (3). Experimental and fitted rates are compared in Figure 7. The R^2- and tangent-values refer to the linear regression between experimental and fitted rates.

Metal	k_{DMA}	a	k_{asc}	b	k_{syn}	c	d	R^2	Tangent
	(s^{-1})		(s^{-1})		($L\ s^{-1}\ mol^{-1}$)				
Fe	9.8×10^{-8}	0.37	n.d.	n.d.	4.4×10^{-3}	0.56	1	0.997	1.00
Ni	3.8×10^{-6}	0.91	n.d.	n.d.	1.4×10^{-4}	0.39	1	0.993	0.99
Co	n.d.	n.d.	n.d.	n.d.	4.9×10^{-5}	0.16	1	0.995	1.00
Mn	n.d.	n.d.	5.6×10^{-4} (3.3×10^{-5}) #	1.37 (1) #	n.d.	n.d.	1	0.996 (0.97)	1.03 (1.20)
Cu	4.9×10^{-8}	0.32	n.d.	n.d.	n.d.	n.d.	n.d.	0.98	1.06
Zn	5.2×10^{-8}	0.36	n.d.	n.d.	n.d.	n.d.	n.d.	0.91	0.97

n.d.: Not determined; # values between brackets are from a fit of the rate data from the *varying reductant concentration experiment* in which the rate order was fixed at 1.

Because the rate orders a and c differ among metals, differences in rate constants k_{DMA} and k_{syn} cannot be directly interpreted in terms of differences in mobilization rates. All values for a and c were between 0 and 1, where 0 represents a *DMA* concentration independent mobilization rate, and 1 represents a linear increase in mobilization rate with increasing *DMA* concentration. The a-values for Fe, Zn and Cu are within a close range (a = 0.32–0.37), implying a similar, non-linear *DMA* concentration dependency in the mobilization rate (Table 1). For Ni mobilization, with an a-value of 0.91, there is near-linear relation with the *DMA* concentration. In a previous study with Santomera soil, it was hypothesized that *DMA* may mainly mobilize Ni from hydroxide minerals, and Fe, Zn and Cu from SOM [42]. Possibly the difference in rate order is related to a difference in soil constituent from which *DMA* mobilized the metals. For Co and Mn no values for k_{DMA} and a could be determined, due to the low mobilized concentrations in absence of ascorbate.

Reductive dissolution of pure Mn-oxide minerals has been reported to follow first order kinetics in the reductant concentration [61,62]. The rate order for the net reductive dissolution of Mn (b-value) from Santomera soil, however, was larger than 1 (1.37; Table 1). This is potentially related to non-linear back-adsorption of Mn(II) after reduction, particularly for the lower ascorbate concentration range; Mn mobilization in the varying reductant concentration experiment (Figure 3), covering a larger ascorbate concentration range, could be fit better assuming Mn mobilization was first order in ascorbate concentration (Table 1).

The mobilized concentrations (Figure 6) and c-values (Table 1) indicate that synergistic mobilization of competing elements Ni (0.39) and Co (0.16) is less *DMA* concentration dependent than Fe mobilization (0.56). Hence, the relative contribution of Fe to the synergistically mobilized metals will increase with increasing *DMA* concentration. Also, because all a- and c-values are smaller than 1, the time until the free ligand is depleted and competitive Fe displacement sets in becomes longer with increasing *DMA* concentration.

4. Conclusions

Our results demonstrate that it is not required that ligands and reductants are exuded simultaneously for generating synergistic Fe mobilization. Furthermore, in order to maximize the increase in window of Fe uptake through synergistic Fe mobilization, ligand and reductant concentrations need to be matched. In this context, constraints from microbial degradation on the residence time of the phytosiderophore ligands in the rhizosphere and from enhanced mobilization of competing metals (particularly Ni and Co), displacing Fe from Fe-phytosiderophore complexes once the free ligand concentration becomes depleted need to be balanced. How quickly depletion of the free ligand occurs, depends on both the (applied) ligand concentration and the rates of metal complexation. The latter is related to the (applied) reductant concentration. The duration of the synergistic Fe

mobilization increases with increasing phytosiderophore concentration and with decreasing reductant concentrations. The maximum synergistic effect increases with increasing reductant concentrations. The mobilization rate of Fe and competing metals from Santomera soil could be described with a rate law equation (Equation (3)), which was parameterized (Table 1), including contributions from the ligand-only, the reductant-only and a synergistic contribution form ligand and reductant combined.

Our results raise the question if and by what mechanisms plants regulate the matching of exudation of ligands and reductants into the rhizosphere to optimize synergistic Fe mobilization to enlarge the time and concentration window of Fe mobilization and uptake.

Supplementary Materials: The following are available online at http://www.mdpi.com/2571-8789/2/4/67/s1, Table S1: Data from Figure 1, Table S2: Data from Figure 2, Table S3: Data from Figure 3, Table S4: Data from Figure 4, Table S5: Data from Figure 5, Table S6: Data from Figure 6, Table S7: Data from Figure 7, Table S8: Data from Figure A1, Table S9: Data from Figure A2, Table S10: Data from Figure A3, Table S11: Data from Figure A4.

Author Contributions: W.S. conceived and designed the experiments; M.W., C.Z. and W.S. performed the experiments; W.S. and S.K. analyzed the data; W.S. and S.K. wrote the paper.

Funding: This research was funded by the Austrian Science Fund (FWF, Grant No.: I1528-N19 and I2865-N34).

Acknowledgments: We thank Martin Walter (M.W.) and Cornelius Zeller (C.Z) for assistance with the experimental work and acknowledge Christian Stanetty, Martin R. Walter and Paul Kosma from the Division of Organic Chemistry, BOKU for synthesizing the *DMA*.

Conflicts of Interest: The authors declare no conflict of interest.

Appendix A

Table A1. Selected soil properties of Santomera soil; these data have been previously reported by Schenkeveld et al. [16].

			Extraction	
Origin/name	Santomera	CDB	Fe (g kg^{-1})	10.2
Region	Murcia	AmOx	Fe (g kg^{-1})	0.5
Country	Spain	DTPA	Fe (mg kg^{-1})	4.9
Soil classification	entisol		Cu (mg kg^{-1})	1.6
pH $CaCl_2$	7.8		Ni (mg kg^{-1})	0.3
EC (mS cm^{-1})	0.11		Zn (mg kg^{-1})	0.5
SOC (g kg^{-1})	7.3		Co (mg kg^{-1})	0.0
Clay (g kg^{-1})	300		Mn (mg kg^{-1})	3.1
$CaCO_3$ (g kg^{-1})	500			

Appendix B

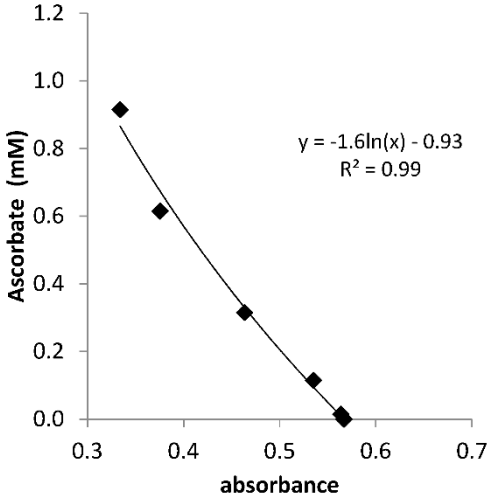

Figure A1. Calibration curve for determining the ascorbate concentration in Santomera soil extract by means of 10 µM methylene blue. Extinction was measured at 665 nm after 60 s of interaction between extract and methylene blue and was corrected for the background (absorbance in soil extract without methylene blue addition). The redox buffer capacity of DOC in the soil extract was also corrected for. LOQ = 0.02 mM.

Table A2. Ascorbate concentration in soil solution as a function of time upon interaction of a 1 mM ascorbate solution with Santomera soil (SSR = 1:10 mM $CaCl_2$; LOQ = 0.02 mM).

Interaction Time (h)	Absorbance	Concentration (mM)
0.083	0.5594	0.022
0.25	0.5616	<0.02
0.5	0.5668	<0.02
1	0.5646	<0.02
4	0.5618	<0.02

Appendix C

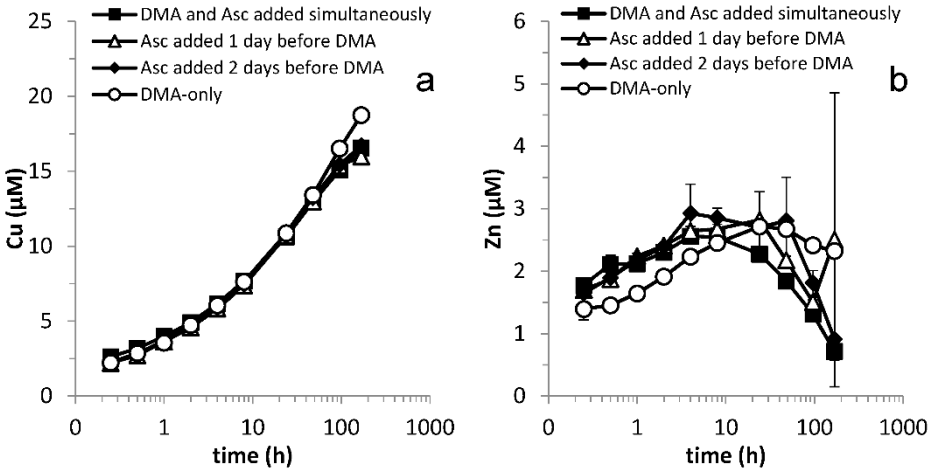

Figure A2. Mobilization of (**a**) Cu and (**b**) Zn from Santomera soil as a function of time by 100 µM *DMA* and 1 mM ascorbate (SSR = 1; 10 mM $CaCl_2$; 0.2 g L^{-1} Bronopol). In combined treatments, *DMA* was applied simultaneously, or one or two days after the ascorbate application. Error bars indicate standard deviations.

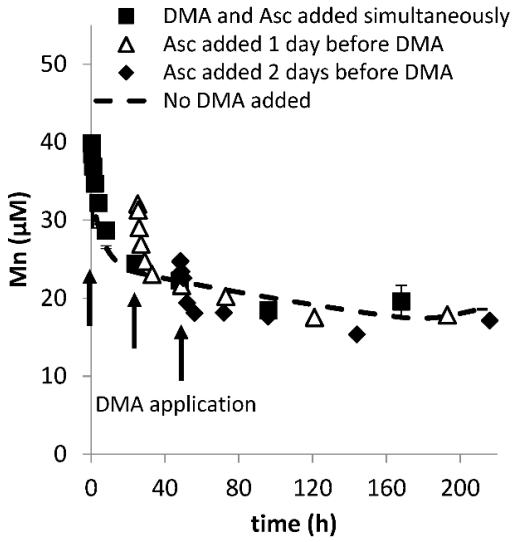

Figure A3. Mobilization of Mn from Santomera soil as a function of time by 100 µM *DMA* and 1 mM ascorbate (SSR = 1; 10 mM $CaCl_2$) in the presence of a sterilant (0.2 g L^{-1} Bronopol). *DMA* was applied either at the same time, or one or two days after ascorbate application. t = 0 corresponds with the moment of ascorbate application. Error bars indicate standard deviations.

Appendix D

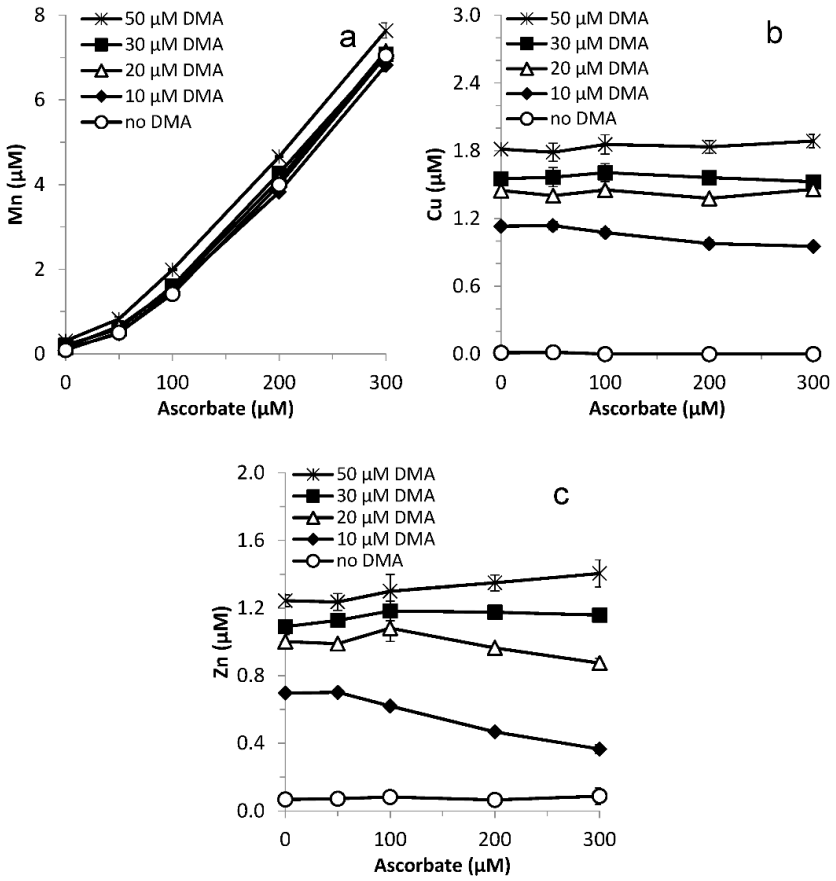

Figure A4. Mobilization of (**a**) Mn, (**b**) Cu and (**c**) Zn from Santomera soil as a function of time by 0, 10 µM, 30 µM, and 100 µM *DMA* in presence and absence of 1 mM ascorbate (SSR = 1; 10 mM $CaCl_2$; 0.2 g L^{-1} Bronopol). Error bars indicate standard deviations.

Appendix E

Table A3. Combinations of *DMA* and ascorbate concentration included for fitting rate constants and rate orders.

	[ascorbate] (μM)				
[*DMA*] (μM)	0	50	100	200	300
10	●				
20	●	●			
30	●	●	●	●	
50	●	●	●	●	●

References

1. Hersman, L.E.; Huang, A.; Maurice, P.A.; Forsythe, J.E. Siderophore production and iron reduction by *Pseudomonas mendocina* in response to iron deprivation. *Geomicrobiol. J.* **2000**, *17*, 261–273. [CrossRef]
2. Marschner, H. *Mineral Nutrition of Higher Plants*, 2nd ed.; Academic Press: London, UK, 1995; p. 889.
3. Lindsay, W.L. *Chemical Equilibria in Soils*; John Wiley and Sons: New York, NY, USA, 1979; p. 449.
4. Mortvedt, J.J. Correcting iron deficiencies in annual and perennial plants: Present technologies and future prospects. *Plant Soil* **1991**, *130*, 273–279. [CrossRef]
5. Martin, J.H.; Fitzwater, S.E. Iron-deficiency limits phytoplankton growth in the northeast pacific subarctic. *Nature* **1988**, *331*, 341–343. [CrossRef]
6. Marschner, H.; Römheld, V.; Kissel, M. Different strategies in higher-plants in mobilization and uptake of iron. *J. Plant Nutr.* **1986**, *9*, 695–713. [CrossRef]
7. Marschner, H.; Römheld, V. Strategies of plants for acquisition of iron. Paper presented at the Seventh International Symposium on Iron Nutrition in Soils and Plants, Zaragoza, Spain, 27 June–2 July 1993; pp. 261–274, 1981 ref.
8. Zinder, B.; Furrer, G.; Stumm, W. The coordination chemistry of weathering II Dissolution of Fe(III) oxides. *Geochim. Cosmochim. Acta* **1986**, *50*, 1861–1869. [CrossRef]
9. Kraemer, S.M. Iron oxide dissolution and solubility in the presence of siderophores. *Aquat. Sci.* **2004**, *66*, 3–18. [CrossRef]
10. Takagi, S.I. Naturally occurring iron-chelating compounds in oat-root and rice-root washings. I. Activity measurement and prelininary characterization. *Soil Sci. Plant Nutr.* **1976**, *22*, 423–433. [CrossRef]
11. Lemanceau, P.; Bauer, P.; Kraemer, S.; Briat, J.F. Iron dynamics in the rhizosphere as a case study for analyzing interactions between soils, plants and microbes. *Plant Soil* **2009**, *321*, 513–535. [CrossRef]
12. Crowley, D.; Kraemer, S.M. Function of Siderophores in the Plant Rhizosphere. In *The Rhizosphere: Biochemistry and Organic Substances at the Soil-Plant Interface*; Pinton, R., Varanini, Z., Nannipieri, P., Eds.; CRC Press: Boca Raton, FL, USA, 2008; p. 616.
13. Kraemer, S.M.; Crowley, D.E.; Kretzschmar, R. Geochemical aspects of phytosiderophore-promoted iron acquisition by plants. In *Advances Agronomy*; Sparks, D.L., Ed.; Elsevier: Amsterdam, The Netherlands, 2006; Volume 91, pp. 1–46.
14. Takagi, S.; Nomoto, K.; Takemoto, T. Physiological aspect of mugineic acid, a possible phytosiderophore of graminaceous plants. *J. Plant Nutr.* **1984**, *7*, 469–477. [CrossRef]
15. Oburger, E.; Gruber, B.; Schindlegger, Y.; Schenkeveld, W.D.C.; Hann, S.; Kraemer, S.M.; Wenzel, W.; Puschenreiter, M. Root exudation of phytosiderophores from soil grown wheat. *New Phytol.* **2014**, *203*, 1161–1174. [CrossRef]
16. Schenkeveld, W.D.C.; Schindlegger, Y.; Oburger, E.; Puschenreiter, M.; Hann, S.; Kraemer, S.M. Geochemical processes constraining iron uptake in strategy II Fe acquisition. *Environ. Sci. Technol.* **2014**, *48*, 12662–12670. [CrossRef] [PubMed]
17. Oburger, E.; Dell'mour, M.; Hann, S.; Wieshammer, G.; Puschenreiter, M.; Wenzel, W.W. Evaluation of a novel tool for sampling root exudates from soil-grown plants compared to conventional techniques. *Environ. Exp. Bot.* **2013**, *87*, 235–247. [CrossRef]

18. Fan, T.W.M.; Lane, A.N.; Pedler, J.; Crowley, D.; Higashi, R.M. Comprehensive analysis of organic ligands in whole root exudates using nuclear magnetic resonance and gas chromatography mass spectrometry. *Anal. Biochem.* **1997**, *251*, 57–68. [CrossRef] [PubMed]
19. Reichard, P.U.; Kraemer, S.M.; Frazier, S.W.; Kretzschmar, R. Goethite dissolution in the presence of phytosiderophores: Rates, mechanisms, and the synergistic effect of oxalate. *Plant Soil* **2005**, *276*, 115–132. [CrossRef]
20. Schenkeveld, W.D.C.; Wang, Z.M.; Giammar, D.E.; Kraemer, S.M. Synergistic Effects between Biogenic Ligands and a Reductant in Fe Acquisition from Calcareous Soil. *Environ. Sci. Technol.* **2016**, *50*, 6381–6388. [CrossRef] [PubMed]
21. Reichard, P.U.; Kretzschmar, R.; Kraemer, S.M. Dissolution mechanisms of goethite in the presence of siderophores and organic acids. *Geochim. Cosmochim. Acta* **2007**, *71*, 5635–5650. [CrossRef]
22. Akafia, M.M.; Harrington, J.M.; Bargar, J.R.; Duckworth, O.W. Metal oxyhydroxide dissolution as promoted by structurally diverse siderophores and oxalate. *Geochim. Cosmochim. Acta* **2014**, *141*, 258–269. [CrossRef]
23. Cheah, S.F.; Kraemer, S.M.; Cervini-Silva, J.; Sposito, G. Steady-state dissolution kinetics of goethite in the presence of desferrioxamine B and oxalate ligands: Implications for the microbial acquisition of iron. *Chem. Geol.* **2003**, *198*, 63–75. [CrossRef]
24. Cervini-Silva, J.; Sposito, G. Steady-state dissolution kinetics of aluminum-goethite in the presence of desferrioxamine-B and oxalate ligands. *Environ. Sci. Technol.* **2002**, *36*, 337–342. [CrossRef]
25. Zhong, L.Y.; Yang, J.W.; Liu, L.M.; Li, X.Y. Desferrioxamine-B promoted dissolution of an Oxisol and the effect of low-molecular-weight organic acids. *Biol. Fertil. Soils* **2013**, *49*, 1077–1083. [CrossRef]
26. Banwart, S.; Davies, S.; Stumm, W. The role of oxalate in accelerating the reductive dissolution of hematite (alpha-Fe_2O_3) by ascorbate. *Colloid Surf.* **1989**, *39*, 303–309. [CrossRef]
27. Wang, Z.M.; Schenkeveld, W.D.C.; Kraemer, S.M.; Giammar, D.E. Synergistic Effect of Reductive and Ligand-Promoted Dissolution of Goethite. *Environ. Sci. Technol.* **2015**, *49*, 7236–7244. [CrossRef] [PubMed]
28. Kang, K.; Schenkeveld, W.D.C.; Biswakarma, J.; Borowski, S.C.; Hug, S.J.; Hering, J.G.; Kraemer, S.M. The catalytic role of low Fe(II) concentrations in ligand-controlled dissolution of Fe(III)(hydr)oxide minerals. *Environ. Sci. Technol.* **2018**. [CrossRef] [PubMed]
29. Biswakarma, J.; Kang, K.; Borowski, S.C.; Schenkeveld, W.D.C.; Kraemer, S.M.; Hering, J.G.; Hug, S.J. Fe(II)-catalzyed ligand-controlled dissolution of iron(hydr)oxides. *Environ. Sci. Technol.* **2018**. [CrossRef]
30. Zuo, Y.M.; Zhang, F.S. Effect of peanut mixed cropping with gramineous species on micronutrient concentrations and iron chlorosis of peanut plants grown in a calcareous soil. *Plant Soil* **2008**, *306*, 23–36. [CrossRef]
31. Xiong, H.C.; Kakei, Y.; Kobayashi, T.; Guo, X.T.; Nakazono, M.; Takahashi, H.; Nakanishi, H.; Shen, H.Y.; Zhang, F.S.; Nishizawa, N.K.; et al. Molecular evidence for phytosiderophore-induced improvement of iron nutrition of peanut intercropped with maize in calcareous soil. *Plant Cell Environ.* **2013**, *36*, 1888–1902. [CrossRef] [PubMed]
32. Marschner, H.; Treeby, M.; Römheld, V. Role of root-induced changes in the rhizosphere for iron acquisition in higher plants. *J. Plant Nutr. Soil Sci.* **1989**, *152*, 197–204. [CrossRef]
33. Dehner, C.; Morales-Soto, N.; Behera, R.K.; Shrout, J.; Theil, E.C.; Maurice, P.A.; Dubois, J.L. Ferritin and ferrihydrite nanoparticles as iron sources for Pseudomonas aeruginosa. *J. Biol. Inorg. Chem.* **2013**, *18*, 371–381. [CrossRef]
34. Vartivarian, S.E.; Cowart, R.E. Extracellular iron reductases: Identification of a new class of enzymes by siderophore-producing microorganisms. *Arch. Biochem. Biophys.* **1999**, *364*, 75–82. [CrossRef]
35. Schmidt, H.; Gunther, C.; Weber, M.; Sporlein, C.; Loscher, S.; Bottcher, C.; Schobert, R.; Clemens, S. Metabolome Analysis of Arabidopsis thaliana Roots Identifies a Key Metabolic Pathway for Iron Acquisition. *PLoS ONE* **2014**, *9*, e102444. [CrossRef]
36. Fourcroy, P.; Siso-Terraza, P.; Sudre, D.; Saviron, M.; Reyt, G.; Gaymard, F.; Abadia, A.; Abadia, J.; Alvarez-Fernandez, A.; Briat, J.F. Involvement of the ABCG37 transporter in secretion of scopoletin and derivatives by Arabidopsis roots in response to iron deficiency. *New Phytol.* **2014**, *201*, 155–167. [CrossRef] [PubMed]
37. Schmid, N.B.; Giehl, R.F.H.; Doll, S.; Mock, H.P.; Strehmel, N.; Scheel, D.; Kong, X.L.; Hider, R.C.; von Wiren, N. Feruloyl-CoA 6′-Hydroxylase1-Dependent Coumarins Mediate Iron Acquisition from Alkaline Substrates in Arabidopsis. *Plant Physiol.* **2014**, *164*, 160–172. [CrossRef] [PubMed]

38. Schenkeveld, W.D.C.; Reichwein, A.M.; Bugter, M.H.J.; Temminghoff, E.J.M.; van Riemsdijk, W.H. Performance of Soil-Applied FeEDDHA Isomers in Delivering Fe to Soybean Plants in Relation to the Moment of Application. *J. Agric. Food Chem.* **2010**, *58*, 12833–12839. [CrossRef] [PubMed]
39. Namba, K.; Murata, Y.; Horikawa, M.; Iwashita, T.; Kusumoto, S. A practical synthesis of the phytosiderophore 2′-deoxymugineic acid: A key to the mechanistic study of iron acquisition by graminaceous plants. *Angew. Chem. Int. Ed.* **2007**, *46*, 7060–7063. [CrossRef] [PubMed]
40. Lopez-Rayo, S.; Di Foggia, M.; Moreira, E.R.; Donnini, S.; Bombai, G.; Filippini, G.; Pisi, A.; Rombola, A.D. Physiological responses in roots of the grapevine rootstock 140 Ruggeri subjected to Fe deficiency and Fe-heme nutrition. *Plant Physiol. Biochem.* **2015**, *96*, 171–179. [CrossRef] [PubMed]
41. Walter, M.; Kraemer, S.M.; Schenkeveld, W.D.C. The effect of pH, electrolytes and temperature on the rhizosphere geochemistry of phytosiderophores. *Plant Soil* **2017**, *418*, 5–23. [CrossRef] [PubMed]
42. Schenkeveld, W.D.C.; Kimber, R.L.; Walter, M.; Oburger, E.; Puschenreiter, M.; Kraemer, S.M. Experimental considerations in metal mobilization from soil by chelating ligands: The influence of soil-solution ratio and pre-equilibration—A case study on Fe acquisition by phytosiderophores. *Sci. Total Environ.* **2017**, *579*, 1831–1842. [CrossRef] [PubMed]
43. Puschenreiter, M.; Gruber, B.; Wenzel, W.W.; Schindlegger, Y.; Hann, S.; Spangl, B.; Schenkeveld, W.D.C.; Kraemer, S.M.; Oburger, E. Phytosiderophore-induced mobilization and uptake of Cd, Cu, Fe, Ni, Pb and Zn by wheat plants grown on metal-enriched soils. *Environ. Exp. Bot.* **2017**, *138*, 67–76. [CrossRef]
44. Manceau, A.; Drits, V.A.; Silvester, E.; Bartoli, C.; Lanson, B. Structural mechanism of Co^{2+} oxidation by the phyllomanganate buserite. *Am. Miner.* **1997**, *82*, 1150–1175. [CrossRef]
45. Peacock, C.L. Physiochemical controls on the crystal-chemistry of Ni in birnessite: Genetic implications for ferromanganese precipitates. *Geochim. Cosmochim. Acta* **2009**, *73*, 3568–3578. [CrossRef]
46. Post, J.E. Manganese oxide minerals: Crystal structures and economic and environmental significance. *Proc. Natl. Acad. Sci. USA* **1999**, *96*, 3447–3454. [CrossRef] [PubMed]
47. Morgan, J.J. Kinetics of reaction between O_2 and Mn(II) species in aqueous solutions. *Geochim. Cosmochim. Acta* **2005**, *69*, 35–48. [CrossRef]
48. Handler, R.M.; Beard, B.L.; Johnson, C.M.; Scherer, M.M. Atom Exchange between Aqueous Fe(II) and Goethite: An Fe Isotope Tracer Study. *Environ. Sci. Technol.* **2009**, *43*, 1102–1107. [CrossRef]
49. Frierdich, A.J.; Catalano, J.G. Controls on Fe(II)-Activated Trace Element Release from Goethite and Hematite. *Environ. Sci. Technol.* **2012**, *46*, 1519–1526. [CrossRef] [PubMed]
50. Frierdich, A.J.; Catalano, J.G. Fe(II)-Mediated Reduction and Repartitioning of Structurally Incorporated Cu, Co, and Mn in Iron Oxides. *Environ. Sci. Technol.* **2012**, *46*, 11070–11077. [CrossRef] [PubMed]
51. Chen, C.M.; Thompson, A. Ferrous Iron Oxidation under Varying pO(2) Levels: The Effect of Fe(III)/Al(III) Oxide Minerals and Organic Matter. *Environ. Sci. Technol.* **2018**, *52*, 597–606. [CrossRef]
52. Baltpurvins, K.A.; Burns, R.C.; Lawrance, G.A.; Stuart, A.D. Effect of pH and anion type on the aging of freshly precipitated iron(III) hydroxide sludges. *Environ. Sci. Technol.* **1996**, *30*, 939–944. [CrossRef]
53. ThomasArrigo, L.K.; Mikutta, C.; Byrne, J.; Kappler, A.; Kretzschmar, R. Iron(II)-Catalyzed Iron Atom Exchange and Mineralogical Changes in Iron-rich Organic Freshwater Flocs: An Iron Isotope Tracer Study. *Environ. Sci. Technol.* **2017**, *51*, 6897–6907. [CrossRef] [PubMed]
54. Xiao, W.; Jones, A.M.; Collins, R.N.; Waite, T.D. Investigating the effect of ascorbate on the Fe(II)-catalyzed transformation of the poorly crystalline iron mineral ferrihydrite. *Biochim. Biophys. Acta-Gen. Subj.* **2018**, *1862*, 1760–1769. [CrossRef] [PubMed]
55. Tamura, H.; Kawamura, S.; Hagayama, M. Acceleration of the oxidation of Fe^{2+} ions by Fe(III)-oxyhydroxides. *Corros. Sci.* **1980**, *20*, 963–971. [CrossRef]
56. Oburger, E.; Gruber, B.; Wanek, W.; Watzinger, A.; Stanetty, C.; Schindlegger, Y.; Hann, S.; Schenkeveld, W.D.C.; Kraemer, S.M.; Puschenreiter, M. Microbial decomposition of ^{13}C- labeled phytosiderophores in the rhizosphere of wheat: Mineralization dynamics and key microbial groups involved. *Soil Biol. Biochem.* **2016**, *98*, 196–207. [CrossRef]
57. Schenkeveld, W.D.C.; Oburger, E.; Gruber, B.; Schindlegger, Y.; Hann, S.; Puschenreiter, M.; Kraemer, S.M. Metal mobilization from soils by phytosiderophores—Experiment and equilibrium modeling. *Plant Soil* **2014**, *383*, 59–71. [CrossRef] [PubMed]
58. Simanova, A.A.; Pena, J. Time-Resolved Investigation of Cobalt Oxidation by Mn(III)-Rich delta-MnO_2 Using Quick X-ray Absorption Spectroscopy. *Environ. Sci. Technol.* **2015**, *49*, 10867–10876. [CrossRef] [PubMed]

59. Walter, M.; Oburger, E.; Schindlegger, Y.; Hann, S.; Puschenreiter, M.; Kraemer, S.M.; Schenkeveld, W.D.C. Retention of phytosiderophores by the soil solid phase—Adsorption and desorption. *Plant Soil* **2016**. [CrossRef] [PubMed]
60. Römheld, V. The role of phytosiderophores in acquisition of iron and other micronutrients in graminaceous species—An ecological approach. *Plant Soil* **1991**, *130*, 127–134. [CrossRef]
61. Matocha, C.J.; Sparks, D.L.; Amonette, J.E.; Kukkadapu, R.K. Kinetics and mechanism of birnessite reduction by catechol. *Soil Sci. Soc. Am. J.* **2001**, *65*, 58–66. [CrossRef]
62. Stone, A.T.; Morgan, J.J. Reduction and dissolution of manganese(III) and manganese(IV) oxides by organics 1. reaction with hydroquinone. *Environ. Sci. Technol.* **1984**, *18*, 450–456. [CrossRef]